JCB Article

Dictyostelium cell death: early emergence and demise of highly polarized paddle cells

Jean-Pierre Levraud,[1] Myriam Adam,[1] Marie-Françoise Luciani,[1] Chantal de Chastellier,[1] Richard L. Blanton,[2] and Pierre Golstein[1]

[1]Centre d'Immunologie de Marseille-Luminy, Institut National de la Santé et de la Recherche Medicale/Centre National de la Recherche Scientifique, Case 906, Parc Scientifique de Luminy, 13288 Marseille Cedex 9, France
[2]Department of Biological Sciences, Texas Tech University, Lubbock, TX 79409

Cell death in the stalk of *Dictyostelium discoideum*, a prototypic vacuolar cell death, can be studied in vitro using cells differentiating as a monolayer. To identify early events, we examined potentially dying cells at a time when the classical signs of *Dictyostelium* cell death, such as heavy vacuolization and membrane lesions, were not yet apparent. We observed that most cells proceeded through a stereotyped series of differentiation stages, including the emergence of "paddle" cells showing high motility and strikingly marked subcellular compartmentalization with actin segregation. Paddle cell emergence and subsequent demise with paddle-to-round cell transition may be critical to the cell death process, as they were contemporary with irreversibility assessed through time-lapse videos and clonogenicity tests. Paddle cell demise was not related to formation of the cellulose shell because cells where the cellulose-synthase gene had been inactivated underwent death indistinguishable from that of parental cells. A major subcellular alteration at the paddle-to-round cell transition was the disappearance of F-actin. The *Dictyostelium* vacuolar cell death pathway thus does not require cellulose synthesis and includes early actin rearrangements (F-actin segregation, then depolymerization), contemporary with irreversibility, corresponding to the emergence and demise of highly polarized paddle cells.

Introduction

In animal cells, programmed cell death leads in many cases to characteristic "apoptotic" lesions (Kerr et al., 1972), and is often dependent on activation of a particular class of cysteine proteases called caspases (Ellis and Horvitz, 1986; Shi, 2002). There are also nonapoptotic types of cell death in vertebrates, often necrotic or vacuolar (Searle et al., 1982; Clarke, 1990; Schwartz et al., 1993; Zakeri et al., 1995; Chautan et al., 1999; Fiers et al., 1999; Kitanaka and Kuchino, 1999), at least some of which are caspase-independent and mechanistically still incompletely defined (Kitanaka and Kuchino, 1999; Leist and Jaattela, 2001). Although molecular studies of caspase-dependent cell death benefited tremendously from the availability of the *Caenorhabditis elegans* model system, there is currently no very good similar model organism for caspase-independent cell death (however, see recent reports in *C. elegans* itself; Chung et al., 2000; Xu et al., 2001; Syntichaki et al., 2002).

Among extant eukaryotic organisms undergoing development and showing cell death, the slime mold *Dictyostelium discoideum* is one of the simplest, having emerged earliest in evolution (about one billion years ago, apparently before the divergence to animals and fungi; Baldauf et al., 2000), and presents marked genetic advantages such as haploidy, a small genome, the sequencing of which is currently under completion, and the applicability of several reverse genetic methods enabling direct links between functions and genes (Mann et al., 1998; Kessin, 2001; Glockner et al., 2002). *Dictyostelium* multiplies as a unicellular microorganism when food is abundant, but undergoes development on starvation: cells aggregate and differentiate, morphogenesis leads first to a migrating slug, then to a fruiting body with a mass of spores at the tip of a stalk composed of dead cells (Whittingham and Raper, 1960). On a practical front, methods exist to trigger differentiation in vitro without morphogenesis, in particular using *Dictyostelium* cells of the HMX44A substrain, leading to cells dying as a monolayer (Kay, 1987; Cornillon et al., 1994) that are easier to study than cells in a stalk.

The online version of this article includes supplemental material.

Address correspondence to Pierre Golstein, Centre d'Immunologie de Marseille-Luminy, INSERM/CNRS, Case 906, Parc Scientifique de Luminy, 13288 Marseille Cedex 9, France. Tel.: 33-4-91-26-94-68. Fax: 33-4-91-26-94-30. E-mail: golstein@ciml.univ-mrs.fr

Key words: cell death; *Dictyostelium*; actin; cellulose; cell polarity

The Journal of Cell Biology, Volume 160, Number 7, March 31, 2003 1105–1114
http://www.jcb.org/cgi/doi/10.1083/jcb.200212104

Supplemental material can be found at:
http://doi.org/10.1083/jcb.200212104

A previous report focused mostly on the "end product" aspect of this cell death: ~20–24 h after induction, cells displayed massive vacuolization, cytoplasmic condensation, a degree of chromatin condensation, delayed plasma membrane disruption, and no DNA fragmentation (Cornillon et al., 1994) as also shown recently in stalks (Kawli et al., 2002). No conventional caspase seemed to play a role in *Dictyostelium* cell death (Olie et al., 1998), and in any case, no caspase gene could be found in the *Dictyostelium* genome (Uren et al., 2000). Another report added in particular the notion that late events included mitochondrial alterations (Arnoult et al., 2001). Early, prevacuolar cell death events may provide insights into and suggest approaches to the study of initial molecular lesions in this cell death. Studying early stages of the *Dictyostelium* cell death pathway, long before detectable onset of vacuolization, we observed in particular the emergence of morphologically distinctive cells (called "paddle" cells) showing strong polarization including a marked segregation of their F-actin network. The subsequent paddle-to-round cell transition was not related to cellulose shell formation as shown through cellulose synthase gene disruption, and occurred at the same time as clear-cut actin depolymerization.

Results

DIF-1 addition triggers a succession of morphological stages including paddle cells

HMX44A cells on starvation synthesize little or none of the stalk cell–inducing factor DIF-1, but they do remain sensitive to it (Kay, 1998). Addition of DIF-1 to cells in rich medium has no effect (unpublished data). Starvation in the absence of exogenous DIF-1 led to flat cells with filopodia (see below) that do not vacuolize and do not die for several days, although interestingly, they show autophagic bodies (Cornillon et al., 1994). Sequential addition of DIF-1 after initiation of starvation leads to death. These initial results showed that *Dictyostelium* cell death in this system (1) requires both starvation and DIF-1 (Kay, 1987; Cornillon et al., 1994); and (2) involves more than just starvation-induced autophagy. Successive cellular stages after starvation and addition of the differentiation factor DIF-1 are shown below in figures and also in videos from which some of the figures have been extracted.

Vegetative cells growing in rich medium (Fig. 1 a and Video 1, available at http://www.jcb.org/cgi/content/full/jcb.200212104) were transferred to starvation medium SB containing 3 mM cAMP, in which they were incubated for 8 h. Control groups were then further incubated in SB alone, leading to a majority of cells with flat body and filopodia (Fig. 1 b and Video 2) that can survive as such for several days. In contrast, incubation in SB in the presence of DIF-1 led to the emergence within 8–16 h of very motile and strikingly compartmentalized cells that we call paddle cells (Fig. 1 c and Videos 3–7; see below). These stop moving within 15–26 h and change morphology to round cells (Fig. 1 d and Video 8). Round cells then progress toward massive vacuolization (Fig. 1 e and Videos 9–11) and still later to rupture of the cytoplasmic membrane (Video 12), which allows propidium iodide staining of the cell remnant

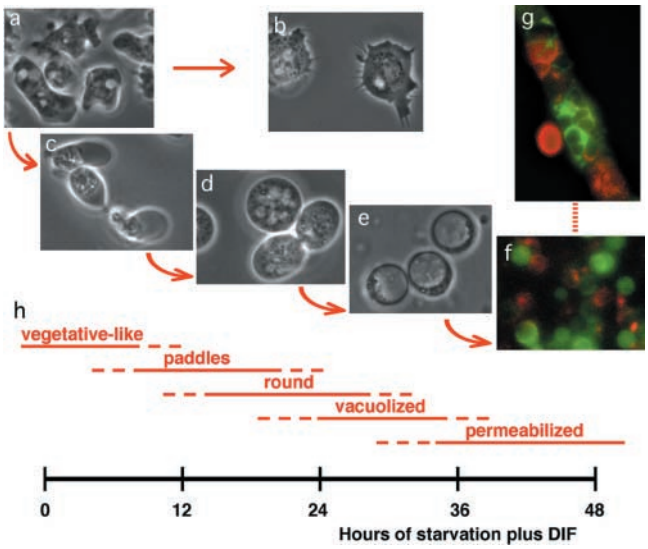

Figure 1. **Diverse cell aspects along *Dictyostelium* terminal differentiation to cell death.** (a) HMX44A *Dictyostelium* cells vegetatively growing in rich medium, or (b) after 8 h of incubation in starvation saline SB in the presence of an excess of cAMP. Many cells have acquired a flat morphology with a number of filopodia, and can keep this morphology for days on further incubation in SB medium. (c) The differentiation factor DIF-1 added to SB induces a sequence of other morphological changes. After 8 to 16 h, many cells acquire a paddle shape (d) that transforms into a round shape. (e) Round cells vacuolize, (f) then progressively, many of the vacuolated cells undergo membrane permeabilization and thus fluoresce red when incubated with propidium iodide, whereas cells with still intact membrane fluoresce green on incubation in a fluorescein diacetate solution. At 48 h, about half of the cells fluoresce red. (g) At 48 h of development, some stalks of fully developed AX2 fruiting bodies also show cells fluorescing red or green, often with an alternate pattern. (h) Approximate time scale of terminal differentiation and death, as reflected by sequential morphological changes, of HMX44A *Dictyostelium* cells subjected to starvation medium and receiving DIF-1 at time zero. There is marked heterogeneity between cells in terms of time to access a given aspect and duration of time with a given aspect.

(Cornillon et al., 1994). Incubation with propidium iodide leads to <50% of the cells fluorescing red after 2 d of starvation and DIF-1, whereas most of the other cells still stain green due to live-cell labeling with fluorescein diacetate (Fig. 1 f). Thus, more than two days are required in vitro (i.e., in submerged monolayers) for half of the cells to die, using this "morphological" criterion for cell death. In vivo (i.e., during normal development), developing *Dictyostelium* AX2 cells in stalks would also stain early with fluorescein diacetate and later with propidium iodide, although we found considerable interstalk variation in the timing of this shift in staining. After 2 d of starvation, stalks often contained areas of cells labeled with fluorescein diacetate alternating with areas of cells labeled with propidium iodide (Fig. 1 g). *Dictyostelium* developmental cell death in vivo thus includes late permeabilization to propidium iodide. Altogether, both in vivo in stalks and in vitro in monolayers, in terms of permeabilization of the plasma membrane death of 50% of the cells requires at least two days. Microscopic examination and numerous time-lapse movies (unpublished data) led to the establishment of an approximate time scale for these various

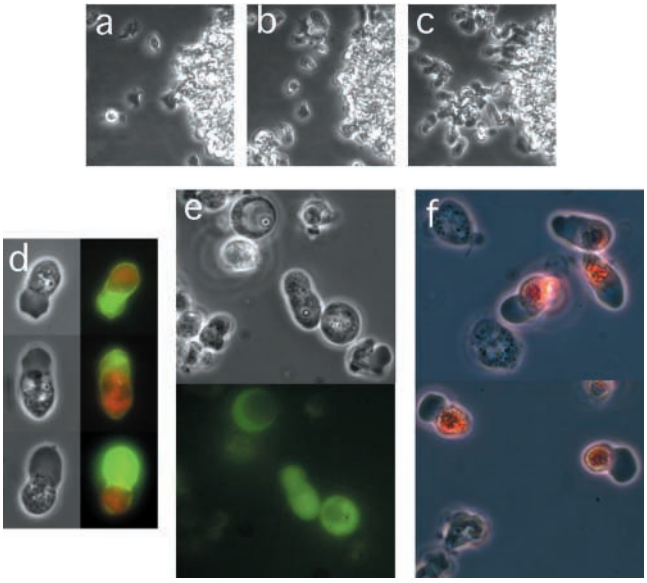

Figure 2. **Paddle cells, emergence, and preliminary characterization.** (a–c) Emergence from a cell clump at 9.5, 10, and 10.5 h, respectively, after addition of DIF-1. (d) Three paddle cells 15 h after addition of DIF-1. Phase contrast (left) or fluorescence microscopy (right) after double staining, with CMXRos labeling (red) the mitochondria in the organelle-rich posterior region of the paddle cells, and with phalloidin labeling (green) the actin-rich propodia. (e) HMX44A cells transfected with ecmA::GFP 16 h after addition of DIF-1, examined by phase contrast (top) or fluorescence (bottom). The paddle cell almost in the middle of the field is among the most fluorescent cells. (f) Two-phase contrast microscopy fields of Neutral Red–stained cells 16 h after addition of DIF-1, exemplifying the fact that most paddle cells are stained and most other cells are not.

cell aspects (Fig. 1 h), which often overlap within a cell population due to marked heterogeneity between cells as to the starting time and duration of a given stage.

Videos also show additional morphological features of this pathway. Thus, quite often, cells rounding up and vacuolizing could be seen to expel material (Videos 8–10; Arnoult et al., 2001), perhaps because of the increase in intracellular pressure due to the accumulation of fluid within the vacuoles. These extrusions could be interpreted as bursting out of cytoplasmic material through the outer cell layers. These include the peripheral actin rim, whose weakening might have consequences somewhat similar to blebbing in apoptotic animal cells, and the neo-synthesized cellulose shell, through which openings do occur (see Fig. 5 b). Also, a cell often initially presents several vacuoles, of which smaller ones empty into larger ones (Videos 9 and 11).

Paddle cells show striking compartmentalization and social behavior

After addition of DIF-1, starved cells tend to form clumps, out of which paddle cells emerge at 8–16 h (Fig. 2, a–c). A few paddle cells can occasionally be seen in SB only, with no added DIF-1, perhaps related to endogenous production of small amounts of DIF-1 even by these HMX44A cells. Paddle cells morphologically comprise an anterior half (Fig. 2 d and Video 3) that we call propodium. The propodium by phase microscopy looks amorphous and opaque gray, and by fluorescence microscopy is stained by the F-actin–specific stain phalloidin (Fig. 2 d). In marked contrast, the posterior half of paddle cells is heterogenous and contains many of the cell organelles. This posterior half is stained by CMXRos (Fig. 2 d) or by MitoTracker® Green (not depicted) and thus bears mitochondria, and by Neutral Red (Fig. 2 f), a classical lysosomal stain. It also contains the DAPI-stainable nucleus (unpublished data). When a paddle cell evolves into a vacuolized cell, the Neutral Red label is found within the vacuole and progressively decreases in intensity (unpublished data). Contrary to other cells in the same preparations, not only are paddle cells heavily labeled by Neutral Red (Fig. 2 f), but also, in HMX44A cells transfected with GFP under an ecmA promoter, they show induction of GFP (Fig. 2 e), two characteristics of prestalk cells. Most interestingly, morphologically similar (if not identical) cells were identified in vivo in dissociated slug cell populations by Inouye's group (see Fig. 12 in Yoshida and Inouye, 2001). There is consistency between ecmA and Neutral Red positivity of paddle cells classifying them as prestalk cells, their position on a pathway leading to cell death, and the presence of morphologically very similar cells in slugs.

Paddle cells exhibit a marked social behavior, i.e., they often associate in (labile) rosettes (Fig. 3 b and Video 4) and in (less labile) cell chains (Fig. 3 c and Videos 5 and 6). This behavior is due at least in part to the existence in each paddle cell of an adhesive lateral or posterior "hook" that we call

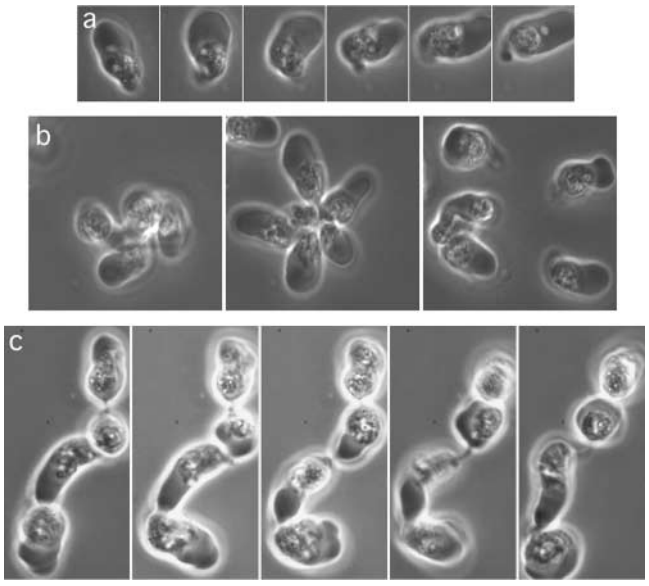

Figure 3. **Paddle cells, social behavior, and parapodia.** (a) A paddle cell on the move 13 h after addition of DIF-1; six images taken 15 s apart. The paddle cell is first moving upwards, then turning to the right. Propodium at the upper part of the cell, then moving to the right. Parapodium first barely visible, then becoming evident, here at the posterior part of the cell. (b) Several paddle cells forming a transient rosette 13 h after addition of DIF-1; three images taken 30 s apart. The third image shows departing paddle cells, with barely visible posterior parapodia. (c) Several paddle cells moving in single line 15 h after addition of DIF-1; five images taken 5 s apart. Parapodia can be seen, first between the upper cell and the second one, then between the second and the third one.

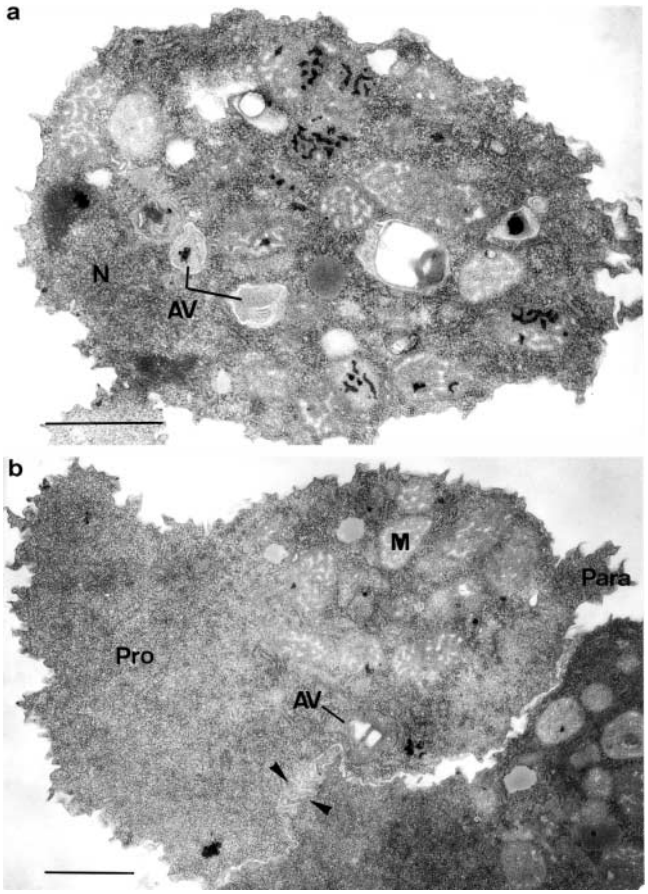

Figure 4. **Ultrastructural appearance of paddle cells.** After 14 h of incubation in SB in the absence or presence of DIF-1, cells were fixed and processed for EM. (a) In most of the cells incubated without DIF-1, the organelles were evenly distributed within the cytoplasm. Note the presence of autophagic vacuoles. (b) Treatment with DIF-1 induced the formation of paddle-shaped cells in which a marked rearrangement of organelles was observed. Dark patches are probably calcium phosphate deposits (de Chastellier and Ryter, 1981). Arrowheads show membrane interdigitations. M, mitochondrion; N, nucleus; AV, autophagic vacuole; Pro, propodium; Para, parapodium. Bars, 1 μm.

parapodium. The parapodium can be seen trailing behind some moving paddle cells (Fig. 3 a and Videos 2–4) or linking cells in chains (Fig. 3 c and Videos 5 and 6) or to the substrate (Video 7). From the examination of paddle cells in a number of videos, we feel that the social behavior of paddle cells may also entail a degree of cytotropism: paddle cells seem to head for, collide, and associate with other cells perhaps more readily than one would expect from chance alone. Whether this is related to chemotactism, and for what, is not known.

Electron microscope observation of paddle cells confirmed a redistribution of organelles. In other cells, organelles are evenly distributed within the cytoplasm (Fig. 4 a). Within paddle cells (Fig. 4 b), mitochondria as well as the scarce endocytic or autophagic vacuoles were all concentrated within the posterior (according to time-lapse videos) one third to one half of the cell. The anterior part of the cell, the propodium, appeared devoid of organelles and contained large amounts of ribosome and glycogen. Due to their abundance and high density, the actin filament network that accumulated within this region as shown by phalloidin staining was difficult to visualize by the EM procedure used in the present paper. The nucleus was often located at the interface between the organelle-free and organelle-rich regions. Small portions of ER were also observed at the interface, and sometimes extended into the organelle-free region. Interestingly, adjacent cells often displayed tight plasma membrane interdigitations, especially at the level of the organelle-free regions. The parapodium, known from the time-lapse studies to have adherent properties, was also poor in organelles and rich in actin.

Most paddle cells are irreversibly committed to death

Previous reports describing *Dictyostelium* cell death dealt mostly with late stages (Cornillon et al., 1994; Arnoult et al., 2001). Our attention was drawn to earlier stages because of results of the following reversibility experiments. First, in clonogenicity tests, cells were subjected to starvation and DIF-1, and immediately cloned by limiting dilution at an average of one cell per well of 96-well microplates. After incubation for various lengths of time to allow multiplication of surviving cells, rich medium was added to each well, leading to growth of countable individual clones quantifying survival. Results were expressed as the proportion of cells able to regrow as a function of the number of hours of incubation in DIF-1 (unpublished data; Fig. 5 c, bottom). After 12 h of incubation, ~50% of the cells were unable to regrow and were thus considered dead by this clonogenic test. This confirms at the clonal level the results obtained earlier at the cell population level (Cornillon et al., 1994). Thus, presumably the same cells, representing ~50% of the cells under test, are clonogenically dead at 12 h, but morphologically dead only after more than two days. Clearly, cells between 12 and 48 h could be considered dead or not depending on the test, i.e., on the definition of death. More immediately useful, these results oriented investigations toward irreversible events taking place within the dying cell at early times (~8–16 h), and committing cells to death before the occurrence of massive vacuolization and long before permeabilization of the cell membrane.

Second, attempts were made to reverse the path of paddle cells toward rounding and vacuolization by shifting back paddle cells to rich medium under the microscope. After 16 h in DIF-1, paddle cells were positioned at the center of a microscope field (oil immersion, 100×) and filmed by time-lapse video. Addition of an excess of rich medium (enough to lead to reversal at very early times; unpublished data) immediately induced the paddle cells to temporarily round up, reflecting the sensitivity of the shape of paddle cells to even moderate local disturbances. After 30–45 min, the cells again showed paddle morphology, and with time either stayed so for several hours of observation, or became round and eventually vacuolized. In no case but one (which we felt afterwards was a not so well-defined paddle cell) out of 13 paddle cells did we see reversal from the paddle morphology. These results, in line with the clonogenicity test above, lead us to conclude that most paddle cells are irreversibly differentiated and engaged on the cell death pathway.

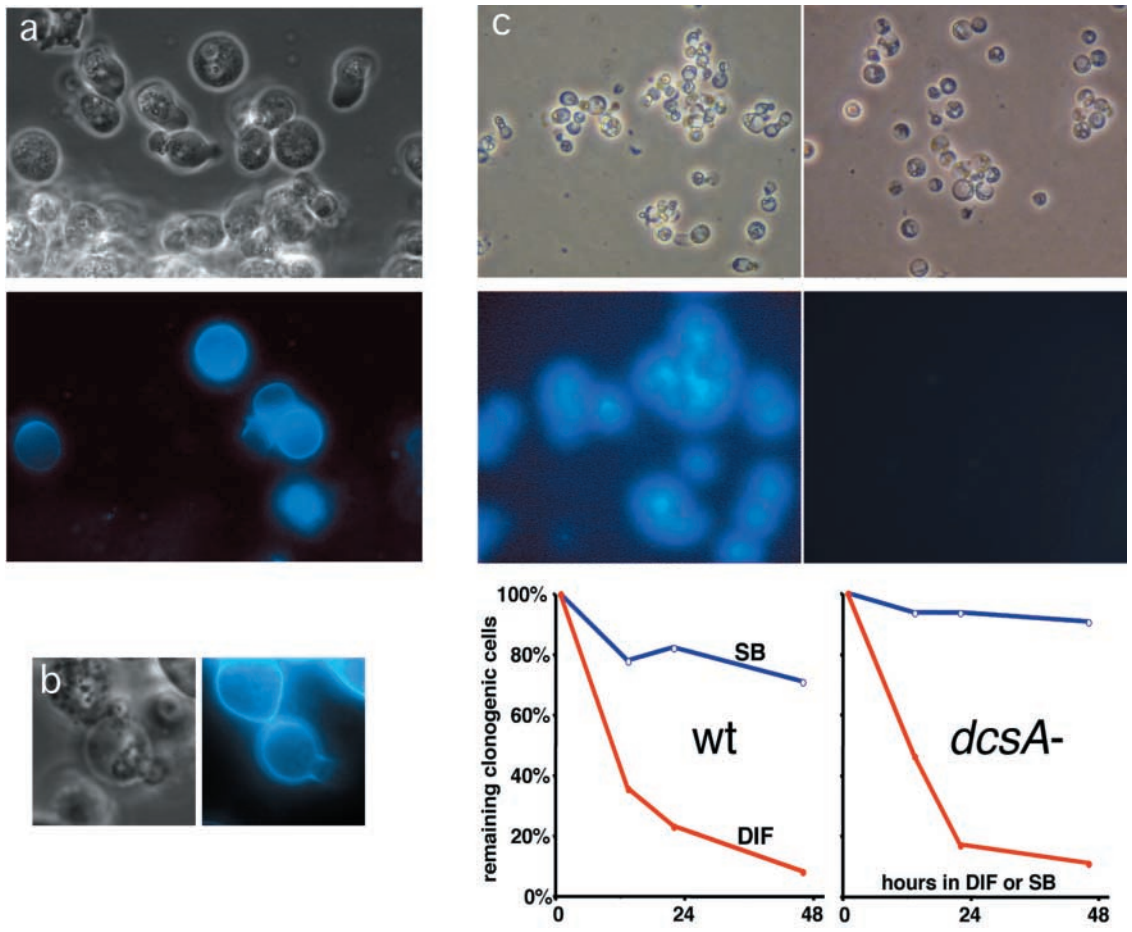

Figure 5. **Cellulose shell appears at the time of, but is not required for, cell rounding.** (a) HMX44A cells 14 h after addition of DIF-1, labeled with Calcofluor. Top, phase contrast; bottom, fluorescence of the same microscopic field. Several round cells are Calcofluor-positive, several paddle cells are not. (b) An HMX44A cell 26 h after addition of DIF-1 showing an opening in its cellulose shell. Left, phase contrast; right, Calcofluor fluorescence. (c) HMX44A wild-type cells (left) and the corresponding cellulose-synthase–deficient (*dcsA*−) cells (right) were incubated in SB and DIF-1 for 47 h, then examined by phase-contrast microscopy (top) or after Calcofluor staining (middle). Also, they were compared as to their clonogenic ability (bottom). The percentage of cells able to regrow on addition of rich medium is indicated as a function of the duration of their initial incubation in SB alone (SB), or in SB plus DIF-1 (DIF). Altogether, the genetic removal of the cellulose shell from *Dictyostelium* cells alters neither other morphological signs of death nor the efficiency of clonogenic death.

The paddle-to-round cell transition: early cellulose encasing is not required for cell death

What mediates the transition from very mobile and differentiated paddle cells to round immobile cells, in a then irreversible pathway to cell death? We considered the possibility that the cellulose shell was at play. Cellulose synthase activity becomes detectable at ~12 h of starvation-induced development in vivo (Blanton, 1993) and is required for accumulation of cellulose. Cellulose can be unambiguously demonstrated after 12–14 h in DIF-1 around some (round) cells using the cellulose stain Calcofluor (Fig. 5 a). That *Dictyostelium* dying cells surround themselves with a cellulose shell suggests that cellulose encasing could be responsible for rounding up and immobilization, and could mechanically prevent cell multiplication, thus accounting for clonogenic death. We took advantage of the existence in *Dictyostelium* of only one gene encoding cellulose synthase (*dcsA*; Blanton et al., 2000), as opposed to the many genes involved in plants. Inactivation of this cellulose synthase gene by homologous recombination in *Dictyostelium* AX4 cells led after development to dilated stalks giving a "snow-man" appearance to fruiting bodies (Blanton et al., 2000). The same homologous recombination construct was used to inactivate the cellulose synthase gene in HMX44 cells. On induction of cell death, Calcofluor, which labeled as expected wild-type cells subjected to starvation and DIF-1, did not label putatively cellulose-synthase–negative cells even after 47 h of incubation in DIF-1 (Fig. 5 c), thus validating the inactivation of the cellulose-synthase gene. When induced to die by starvation and DIF-1, wild-type and cellulose-synthase–inactivated cells showed, after forming similar paddle cells (Video 7), the same pattern of vacuolization, and the same kinetics of clonogenic cell death (Fig. 5 c) as also found in bulk regrowth experiments (unpublished data). Thus, cell death occurs identically by both morphologic and clonogenic criteria, whether or not cellulose encases the dying cells. Clearly, in *Dictyostelium*, the synthesis of cellulose is contemporary to clonogenic cell death, but does not cause it. Instead, both synthesis of cellulose and cell death must have a common trigger downstream of perception of DIF-1. These results

rule out mechanical constraint from the cellulose shell as a significant parameter in *Dictyostelium* cell death.

However, there is one circumstance when cellulose negativity seems to make a difference. Late manifestations of cell death include a decrease in percentage of cells that can be labeled with fluorescein diacetate together with an increase in percentage of cells permeable to propidium iodide (Cornillon et al., 1994). In *dcsA*− cells, on incubation in SB and DIF-1, there is indeed a drop in the number of cells staining with fluorescein diacetate, but there are no detectable cells taking up propidium iodide. At the same time, in a given flask and compared with the initial state of the culture, fewer cells are visible by phase contrast. A likely explanation is that dying *dcsA*− cells, not constrained by any encasing, just disintegrate on disruption of their plasma membrane. This interpretation is comforted by the presence of more debris in *dcsA*− than in wild-type dying cell cultures (unpublished data). This may also be related to the observation in the initial report of *dcsA*− development of late "lysis" of stalk cells (Blanton et al., 2000). If this interpretation is correct, the absence of propidium iodide–positive cells among *dcsA*− dying cells may indicate in turn that, at least in the absence of cellulose, no constraining encasing made of a substance (or substances) other than cellulose prevented disintegration of dying *dcsA*− cells. Altogether, although cellulose encasing may prevent the quick dispersal of dead cell remnants, clearly it is irrelevant to the mechanism of cell death proper in *Dictyostelium*, and in particular to the paddle-to-round cell transition.

The paddle-to-round cell transition is accompanied with actin depolymerization

If not due to an external constraint, then to what is the paddle-to-round cell transition due? This transition was found to be accompanied also with loss of an internal constraint. Namely, round cells were CMXRos-positive, but phalloidin-negative, thus without detectable F-actin (Fig. 6). To quantify this, in a given experiment, cells at 15 h in DIF-1 were photographed and checked for morphology and staining. Of 228 cells, 43 had paddle morphology (about one fifth), and all of these were stained by both CMXRos and phalloidin in a paddle-segregated manner. The remaining 185 cells showed round morphology. Of these round cells, 135 were stained by both CMXRos and phalloidin; however, often with phalloidin staining reduced to a rim, whereas 50 were CMXRos-positive and phalloidin-negative, consistent with a paddle-to-round cell transition accompanied with actin depolymerization. We attempted to document the likely causality relationship between rounding and actin depolymerization by using jasplakinolide or latrunculin A. However, in this system, the toxicity of these drugs rendered interpretation of results difficult (unpublished data).

According to the persistence of at least some CMXRos staining in phalloidin-negative cells, F-actin disappearance would seem to precede massive mitochondrial alteration (reported to occur at ~30 h; Arnoult et al., 2001) and vacuolization. In a cell population evolving somewhat asynchronously, F-actin disappearance may serve as a useful landmark on the cell death pathway at the single-cell level, for instance, in future detailed studies on the state of mitochondria. In addition, among HMX44A cells subjected to starvation and DIF-1, most of the cells showing a Calcofluor-positive cellulose shell were phalloidin-negative or weak (unpublished data). Altogether, at about the same time, the cellulose shell becomes detectable (but irrelevant to death) while actin depolymerizes, cells round up, and evolution to cell death becomes irreversible. Then, the cell proceeds to vacuolization and massive mitochondrial alteration.

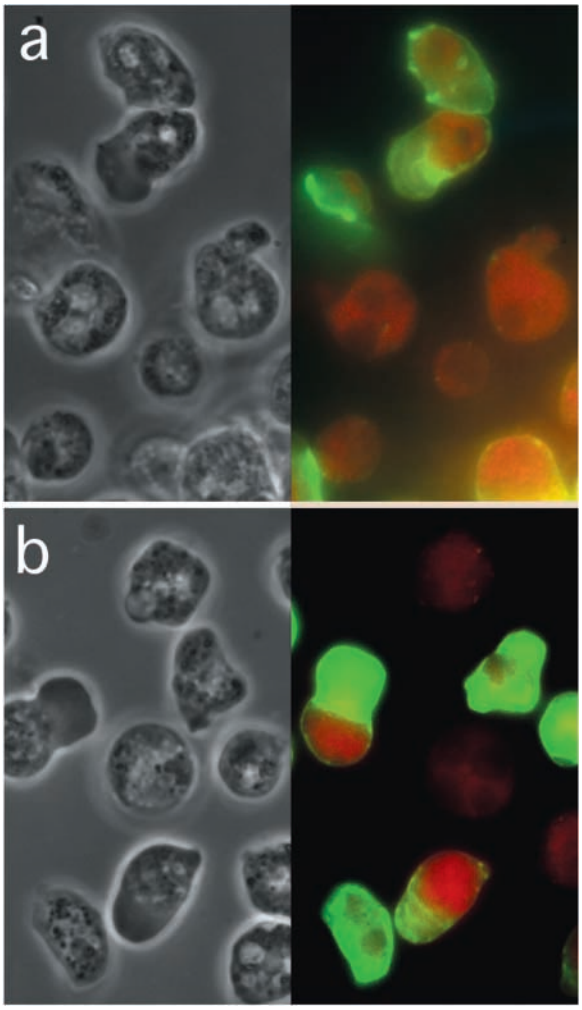

Figure 6. **Cell rounding is accompanied with actin depolymerization.** (a) HMX44A cells 16 h after addition of DIF-1. Left, phase contrast; right, same field stained with CMXRos and phalloidin. Although paddle cells are labeled with both CMXRos (red) and phalloidin (green), a number of round cells are labeled with CMXRos, but not with phalloidin. (b) Another field showing other similar cell patterns.

Discussion

Dictyostelium HMX44 cell death in monolayers includes two successive sets of events. Early events (after paddle cell emergence) include cell immobilization and rounding, loss of clonogenic ability for 50% of the cells 10–12 h after addition of DIF-1, noncausal synthesis of a cellulose shell (this paper), no phosphatidylserine externalization at the plasma membrane (unpublished data), little vacuolization, little membrane permeabilization, a degree of chromatin condensation already induced, however, by starvation without DIF-1, and

no DNA fragmentation (Cornillon et al., 1994). Late events (24–48 h after addition of DIF-1) include massive vacuolization, ring-type annexin staining (unpublished data; Arnoult et al., 2001), cytoplasmic condensation, and very late plasma membrane disruption as shown through videomicroscopy and propidium iodide uptake (Cornillon et al., 1994; this paper). Also, at variance with the early and regular "ladder" type of DNA fragmentation observed in animal cell apoptosis, DNA disintegration in *Dictyostelium* cell death occurs late (after 30 h), and results in an electrophoretic smear rather than in a regular ladder (Cornillon et al., 1994; Arnoult et al., 2001), perhaps as part of the general breakdown of cell components after cell membrane disruption. Late events are clearly consequences rather than initial cause of death.

Our previous work with caspase inhibitors (Olie et al., 1998) and the absence of caspase genes in *Dictyostelium* ruled out a caspase-dependent mechanism. Also, the present paper rules out a causal role for cellulose, and more generally makes it unlikely that an external mechanical constraint accounts for cell death. Although cellulose encasing is not required for cell death, it is required in monolayers to limit the disintegration of dead cells (this paper), and in vivo for the structural role that these (stalk) cells play after their death in *Dictyostelium*. This post-death structural role may be similar to that seen in some dead plant or fungus cells, where other glucans can also be found in cell walls, such as callose and chitin, respectively.

Early in the terminal differentiation pathway leading to cell death, paddle cells endowed with remarkable morphology emerge, showing in particular segregation of F-actin. These highly polarized paddle cells are reminiscent of other instances of cell polarity (Dustin, 2002) and might constitute an interesting model to study this polarity. Segregation of F-actin underlies the appearance of the propodium and the parapodium. In part through the adhesive role of the latter, paddle cells show a marked social behavior, often associating as rosettes and cell chains. This behavior, which may reflect similar in vivo properties, may allow so far unexplored cellular interactions.

The observation of prestalk markers in paddle cells (this paper) and the existence of similar cells in slugs (Yoshida and Inouye, 2001) suggest that these paddle cells are in vitro equivalents of in vivo prestalk cells in classical *Dictyostelium* nomenclature. Also, the subsequent in vitro rounding up, irreversibility, cellulose encasing, vacuolization, and membrane permeabilization all have equivalents in stalk cells including the classical report of nonregrowth in rich medium (Whittingham and Raper, 1960). Thus, the in vitro monolayer experimental system shows traits (Cornillon et al., 1994; this paper) similar to those of starvation-triggered developmental cell death in stalks, strengthening its validity as a model thereof. However, although under our conditions in submerged monolayers, addition of DIF-1 is required for triggering normal-looking cell death, cell death can occur in normal development in the absence of DIF-1 (Thompson and Kay, 2000). From another point of view, the variety of distinctive aspects in *Dictyostelium* differentiation, even considering only this stalk cell pathway, is quite striking.

The paddle-to-round cell transition is accompanied with disappearance of F-actin. This disappearance could reflect depolymerization of intact monomers or cleavage of monomers leading to depolymerization. In the cytoskeleton, many molecules interact with actin and could be involved in such events, also in *Dictyostelium* cells (Lee et al., 2001). In animal apoptotic cell death, rounding up (and often blebbing) is a common and early event, and is usually believed to be due to actin alterations. Although in vitro actin can be directly cleaved by activated caspases (Kayalar et al., 1996; Mashima et al., 1997), current understanding is that caspases activate calpain, which in turn can cleave actin (Brown et al., 1997; Villa et al., 1998). Activation of calpain is itself indirect, through cleavage by activated caspases of Gas2 (Brancolini et al., 1995; Benetti et al., 2001) or calpastatin (Porn-Ares et al., 1998) which thus lose their calpain-inhibitory activity. Other studies indicate that on death, actin may not be cleaved (Song et al., 1997) but may be otherwise altered. Thus, apoptotic membrane blebbing may be regulated by myosin light chain phosphorylation via the myosin light chain kinase and the Rho-activated serine-threonine kinase (Mills et al., 1998; Coleman et al., 2001; Sebbagh et al., 2001), modulating the interaction of the myosin head with actin. Other reports emphasized the contrasted impact of native or caspase-cleaved gelsolin on actin during apoptosis (Kothakota et al., 1997; Ohtsu et al., 1997). Also, at least in some models of apoptosis, actin transcription seems to be decreased first, followed with actin depolymerization, and only later with the cleavage of a significant amount of actin (Guenal et al., 1997). In some cells, actin depolymerization can act as a cause of Bcl-2–rescuable apoptosis (Martin and Leder, 2001). This is not at variance with the results above; it could be that actin alterations are a consequence of early apoptotic events, and are themselves a cause of further downstream events. In this sense, they may constitute a necessary step in the causality chain leading to completion of cell death. Whether this is true for *Dictyostelium* cell death is not known.

Altogether, the various traits of *Dictyostelium* cell death are those of a vacuolar cell death, some of which are reminiscent of vacuolar cell death in animals (Clarke, 1990) or plants (Fukuda, 1997), with only limited resemblance to classical apoptosis. As stated before (Olie et al., 1998), *Dictyostelium* cell death might constitute a model for some instances of caspase-independent vacuolar cell death in higher eukaryotes. Which caspase- and mechanical constraint–independent mechanism is at play in *Dictyostelium* cell death can be further investigated using, e.g., molecular biology approaches (Mann et al., 1998; Levraud et al., 2001) in this genetically tractable organism. More precisely, the early occurrence of loss of clonogenicity provides a temporal basis for this search, showing that causal events should be looked for within the first 10–12 h of death induction, while actin alterations provide mechanistic clues.

Reversibility experiments showed that once cells have become paddle cells, they usually cannot revert to vegetative cells. Moreover, most are then doomed to follow the path to round then to vacuolated cells. At least on the basis of their marked mobility, paddle cells are well alive, whereas the transition from paddle to round cells includes the first visible

destructive events in crippled immobile cells. Thus, with marked reservations due to the current imperfect state of knowledge and of definitions, differentiation to paddle cells might represent an irreversible step in a terminal differentiation pathway, and the paddle-to-round cell transition may already represent a cell death event. In any case, the stereotyped succession of stages in this vacuolar cell death is consistent with the notion of "programmed cell death" in this type of cell death as well as in others, in terms of seemingly reflecting a programmed course of events within the dying cell.

Materials and methods

Cells, cell culture, and light microscopy

D. discoideum axenic strain HMX44A was used for experiments and as recipient strain for cellulose synthase homologous recombination. This strain was cloned from HMX44 cells adapted to axenic growth (a gift from J.G. Williams, University of Dundee, Dundee, UK) that were derived from HM44 mutant cells (Kopachik et al., 1983) originating from V12M2 (Town et al., 1976; Sobolewski et al., 1983; Kay, 1987). HMX44A cells and derivatives were routinely grown at 23°C in HL5 medium (Sussman, 1987) as modified (Cornillon et al., 1994), except for maltose, which was 9 g/l here.

For experiments, unless stated otherwise, vegetative cells in growth phase were washed once and resuspended in HL5 at a concentration of 2×10^5 cells/ml. 1 ml of this cell suspension was distributed in each well of Lab-Tek™ culture chambers (ref. 155380; Nunc). These have a thin glass coverslip bottom allowing high power inverted fluorescence microscopy. After overnight incubation, HL5 was discarded, and each well received 1 ml PBS, pH 6.7 (SB, as in Cornillon et al., 1994), with addition of cAMP to a final concentration of 3 mM. After 8 h of incubation at 22°C in SB and cAMP (Kay, 1987; Cornillon et al., 1994), cells, most of which were then adherent, were washed once in SB and incubated at 22°C in either SB, or SB in the presence of the differentiation factor DIF-1 (Morris et al., 1987; D-3450, Interchim) at a final concentration of 10^{-7} M. After incubation for the indicated period of time, cells in the Lab-Tek™ chambers were treated as follows: for FDA/PI staining, fluoresceine diacetate (F7378, stock solution at 10 mg/ml in acetone; Sigma-Aldrich) was used at a final concentration of 50 μg/ml, and propidium iodide (P4170, stock solution at 53 μg/ml in H_2O; Sigma-Aldrich) was used at a final concentration of 2.6 μg/ml; cells were observed after incubating with these dyes for 10 min. Calcofluor White M2R (F0386, stock solution at 1% wt/vol in H_2O; Sigma-Aldrich) was used at a final concentration of 0.01%, and cells were observed after 5–10 min. For combined CMXRos/phalloidin staining, usually at 14 h after addition of SB and DIF-1, wells containing cells and 1 ml SB plus DIF-1 received MitoTracker® Red CMXRos (M-7512; Molecular Probes, Inc.) to a final concentration of 200 nM for 30 min at 22°C; 0.3 ml PFA 4% in SB was then carefully added; after 10 min at 22°C, cells were washed in SB, and 1 ml SB was added containing 10 μl of a stock solution of Alexa Fluor® 488 phalloidin (A-12379, 300 U in 1.5 ml methanol; Molecular Probes, Inc.); this was followed with overnight incubation.

For Neutral Red staining, vegetative cells were washed in SB and were then subjected to a 0.03% wt/vol solution of Neutral Red (N6634, Sigma-Aldrich) in this phosphate buffer for 5 min; this solution was discarded, and the cells then underwent the usual serial incubations in SB plus cAMP, then SB plus DIF-1.

Cells in Lab-Tek™ chambers were examined using an inverted microscope (Axiovert 200; Carl Zeiss MicroImaging, Inc.), usually at 1,000×. Pictures were taken using a digital camera (AxioCam MRc; Carl Zeiss MicroImaging, Inc.) connected to a PC equipped with Axiovision (Carl Zeiss MicroImaging, Inc.). Images and time-lapse videos were transferred to a Macintosh computer and treated with GraphicConverter.

Processing for EM

Cells grown on hydrophilic petriPERM culture dishes (Sartorius) were prefixed at RT by adding an equal volume of 2.5% glutaraldehyde to the culture medium. After 20 min, the medium was removed and cells were fixed for 1 h at RT with 2.5% glutaraldehyde (grade I; Sigma-Aldrich) in 0.1 M cacodylate buffer (cacodylic acid; Sigma-Aldrich), pH 6.8, containing 0.2 M sucrose, 5 mM $CaCl_2$, and 5 mM $MgCl_2$. Cells were washed overnight at 4°C with sucrose-containing cacodylate buffer, and were then fixed for 1 h at RT with 1% osmium tetroxide (Euromedex) in sucrose-free cacodylate buffer. Cells were then scraped off the culture dishes with a rubber policeman, concentrated in 2% agar in cacodylate buffer, and treated for 1 h at RT with 0.5% uranyl acetate in veronal buffer. Samples were dehydrated in a graded series of acetone and embedded in Epon. Thin sections were stained with 1% uranyl acetate in water and then with lead citrate.

Examination of cells in stalks

Developmentally competent AX2 cells (10^7 cells/100 μl SB) were seeded on nitrocellulose filters (0.8 μm, 47-mm diam, AABP04700; Millipore) kept on 3MM paper (Whatman) soaked with SB. The cells were allowed to undergo development for 24 or 48 h. Each filter was then lightly pressed against a glass slide (LLR2BL SuperFrost® CML; Nemours), allowing some mature fruiting bodies to adhere to the slide. A 100-μl volume of a solution of FDA/PI in SB at the final concentrations indicated above was deposited on the fruiting bodies, a glass coverslip was mounted over this volume, and microscopic examination was done coverslip down.

Clonogenic regrowth assay

HMX44A cells (wt or *dcsA*−) in exponential vegetative growth phase (i.e., between 5×10^5 and 2×10^6 cells/ml) were washed in SB and incubated for 8 h at 22°C in SB plus 3 mM cAMP (typically 10^6 cells in 2.5 ml in a 25-cm^2 flask; Sigma-Aldrich). The supernatant was then carefully removed, fresh SB was added to the flask, and the cells were detached by slamming and flushing. After centrifugation, the pellet was resuspended in SB with repeated pipetting in order to obtain a single-cell suspension before counting. Cells were then distributed in a series of flat-bottom 96-well plates at an average density of one cell/50 μl/well, either in SB alone or in SB plus 10^{-7} M DIF-1. Plates were wrapped in Saran Wrap® to prevent evaporation, and were incubated at 22°C. Regrowth was initiated at a different time point for each plate by adding 150 μl HL5 medium to each well of a given plate, and the plate was incubated for about 10 more days, after which positive wells (containing growing cells) were scored. Based on the Poisson distribution, the total number of clonogenic cells per plate (n) was deduced from the number of positive wells (x) using the following formula: $n = \ln (1 - x/96)/\ln (1 - 1/96)$.

Bulk regrowth assay

HMX44A cells were incubated for 8 h in SB plus cAMP as described above. After cAMP removal, cells were resuspended at 10^5 cells/ml in SB, and 500 μl aliquotes were distributed into a series of wells in 24-well plates, either without or with 10^{-7} M DIF-1. After a variable period of time at 22°C, to initiate regrowth, 1.5 ml HL5 was added to each well. After 48–72 h of additional incubation at 22°C, vegetative cells resulting from regrowth were counted. For each time point of incubation in SB, the percentage of surviving cells in the presence of DIF-1 was deduced from the ratio of cells regrowing after incubation with DIF-1 to that of cells regrowing after incubation in the absence of DIF-1.

Gene inactivation by homologous recombination

For inactivation of the cellulose synthase gene (*dcsA*), a blasticidin-resistance (bsR) cassette was inserted in the BglII site of the *dcsA* coding sequence, resulting in plasmid p*dcsA*-KO (Blanton et al., 2000). This plasmid was restricted to isolate and purify the *dcsA* coding region disrupted by the blasticidin S resistance *bsr* cassette (Sutoh, 1993). HMX44A cells were electrotransfected with 20 μg of this purified DNA, and transfected cells were selected for resistance to 10 μg/ml blasticidin. Blasticidin-resistant cells were cloned by limiting dilution, and 10 clones were Southern blotted to detect homologous recombinants. One clone showed a recombinant hybridization pattern that was also confirmed by PCR analysis, and subsequently, by the absence of Calcofluor-positive material on development.

Online supplemental material

The videos show, in movement, each type of cell mentioned in this paper, and also show transitions in this pathway from one cell type to others. Online supplemental material available at http://www.jcb.org/cgi/content/full/jcb.200212104.

We thank Laurence Aubry, Gérard Klein, and Michel Satre (Commissariat à l'Energie Atomique, Grenoble, France) for helpful discussions, and F. Vanhoutte for performing some of the reversibility experiments. We thank William F. Loomis (University of California, San Diego, San Diego, CA) for the gift of the *dcsA* gene disruption construct, and C. Weijer for helpful discussion.

This work was supported by grants from Institut National de la Santé et de la Recherche Medicale, Centre National de la Recherche Scientifique, Minestere de la Recherche et de la Technologie (Action Concertée Incita-

tive Biologie du Développement et Physiologie Intégrative), and Association pour la Recherche Contre le Cancer . J.-P. Levraud is a Pasteur Institute fellow. M. Adam was supported first by a Training and Mobility of Research Network contract (CEE FMRX CT970153), and then by an European Community Fifth Framework grant (QLG1-CT1999-00739). R.L. Blanton acknowledges support by a grant from the Office of Basic Energy Sciences, U.S. Department of Energy (DE-FG03-99ER20335).

Submitted: 18 December 2002
Revised: 3 February 2003
Accepted: 4 February 2003

References

Arnoult, D., I. Tatischeff, J. Estaquier, M. Girard, F. Sureau, J.P. Tissier, A. Grodet, M. Dellinger, F. Traincard, A. Kahn, et al. 2001. On the evolutionary conservation of the cell death pathway: mitochondrial release of an apoptosis-inducing factor during *Dictyostelium discoideum* cell death. *Mol. Biol. Cell.* 12:3016–3030.

Baldauf, S.L., A.J. Roger, I. Wenk-Siefert, and W.F. Doolittle. 2000. A kingdom-level phylogeny of eukaryotes based on combined protein data. *Science.* 290: 972–977.

Benetti, R., G. Del Sal, M. Monte, G. Paroni, C. Brancolini, and C. Schneider. 2001. The death substrate Gas2 binds m-calpain and increases susceptibility to p53-dependent apoptosis. *EMBO J.* 20:2702–2714.

Blanton, R.L. 1993. Prestalk cells in monolayer cultures exhibit two distinct modes of cellulose synthesis during stalk cell differentiation in *Dictyostelium. Development.* 119:703–710.

Blanton, R.L., D. Fuller, N. Iranfar, M.J. Grimson, and W.F. Loomis. 2000. The cellulose synthase gene of *Dictyostelium*. *Proc. Natl. Acad. Sci. USA.* 97: 2391–2396.

Brancolini, C., M. Benedetti, and C. Schneider. 1995. Microfilament reorganization during apoptosis: The role of Gas2, a possible substrate for ICE-like proteases. *EMBO J.* 14:5179–5190.

Brown, S.B., K. Bailey, and J. Savill. 1997. Actin is cleaved during constitutive apoptosis. *Biochem. J.* 323:233–237.

Chautan, C., G. Chazal, F. Cecconi, P. Gruss, and P. Golstein. 1999. Interdigital cell death can occur through a necrotic and caspase-independent pathway. *Curr. Biol.* 9:967–970.

Chung, S., T.L. Gumienny, M.O. Hengartner, and M. Driscoll. 2000. A common set of engulfment genes mediates removal of both apoptotic and necrotic cell corpses in *C. elegans*. *Nat. Cell Biol.* 2:931–937.

Clarke, P.G. 1990. Developmental cell death: morphological diversity and multiple mechanisms. *Anat. Embryol (Berl).* 181:195–213.

Coleman, M.L., E.A. Sahai, M. Yeo, M. Bosch, A. Dewar, and M.F. Olson. 2001. Membrane blebbing during apoptosis results from caspase-mediated activation of ROCK I. *Nat. Cell Biol.* 3:339–345.

Cornillon, S., C. Foa, J. Davoust, N. Buonavista, J.D. Gross, and P. Golstein. 1994. Programmed cell death in *Dictyostelium*. *J. Cell Sci.* 107:2691–2704.

de Chastellier, C., and A. Ryter. 1981. Calcium-dependent deposits at the plasma membrane of *Dictyostelium discoideum* and their possible relation with contractile proteins. *Biol. Cell.* 40:109–118.

Dustin, M.L. 2002. Shmoos, rafts, and uropods– the many facets of cell polarity. *Cell.* 110:13–18.

Ellis, H.M., and H.R. Horvitz. 1986. Genetic control of programmed cell death in the nematode *C. elegans*. *Cell.* 44:817–829.

Fiers, W., R. Beyaert, W. Declercq, and P. Vandenabeele. 1999. More than one way to die: apoptosis, necrosis and reactive oxygen damage. *Oncogene.* 18: 7719–7730.

Fukuda, H. 1997. Programmed cell death during vascular system formation. *Cell Death Differ.* 4:684–688.

Glockner, G., L. Eichinger, K. Szafranski, J.A. Pachebat, A.T. Bankier, P.H. Dear, R. Lehmann, C. Baumgart, G. Parra, J.F. Abril, et al. 2002. Sequence and analysis of chromosome 2 of *Dictyostelium discoideum*. *Nature.* 418:79–85.

Guenal, I., Y. Risler, and B. Mignotte. 1997. Down-regulation of actin genes precedes microfilament network disruption and actin cleavage during p53-mediated apoptosis. *J. Cell Sci.* 110:489–495.

Kawli, T., B.R. Venkatesh, P.K. Kennady, G. Pande, and V. Nanjundiah. 2002. Correlates of developmental cell death in *Dictyostelium discoideum*. *Differentiation.* 70:272–281.

Kay, R.R. 1987. Cell differentiation in monolayers and the investigation of slime mold morphogens. *Methods Cell Biol.* 28:433–448.

Kay, R.R. 1998. The biosynthesis of differentiation-inducing factor, a chlorinated signal molecule regulating *Dictyostelium* development. *J. Biol. Chem.* 273: 2669–2675.

Kayalar, C., T. Ord, M.P. Testa, L.T. Zhong, and D.E. Bredesen. 1996. Cleavage of actin by interleukin 1 beta-converting enzyme to reverse DNase I inhibition. *Proc. Natl. Acad. Sci. USA.* 93:2234–2238.

Kerr, J.F.R., A.H. Wyllie, and A.R. Currie. 1972. Apoptosis: a basic biological phenomenon with wide-ranging implications in tissue kinetics. *Br. J. Cancer.* 26:239–257.

Kessin, R.H. 2001. Dictyostelium: Evolution, Cell Biology, and the Development of Multicellularity. Cambridge University Press, Cambridge. 300 pp.

Kitanaka, C., and Y. Kuchino. 1999. Caspase-independent programmed cell death with necrotic morphology. *Cell Death Differ.* 6:508–515.

Kopachik, W., A. Oohata, B. Dhokia, J.J. Brookman, and R.R. Kay. 1983. *Dictyostelium* mutants lacking DIF, a putative morphogen. *Cell.* 33:397–403.

Kothakota, S., T. Azuma, C. Reinhard, A. Klippel, J. Tang, K. Chu, T.J. McGarry, M.W. Kirschner, K. Koths, D.J. Kwiatkowski, and L.T. Williams. 1997. Caspase-3-generated fragment of gelsolin: effector of morphological change in apoptosis. *Science.* 278:294–298.

Lee, E., K. Pang, and D. Knecht. 2001. The regulation of actin polymerization and cross-linking in *Dictyostelium*. *Biochim. Biophys. Acta.* 1525:217–227.

Leist, M., and M. Jaattela. 2001. Four deaths and a funeral: from caspases to alternative mechanisms. *Nat. Rev. Mol. Cell Biol.* 2:589–598.

Levraud, J.-P., M. Adam, S. Cornillon, and P. Golstein. 2001. Methods to study cell death in *Dictyostelium discoideum*. *Methods Cell Biol.* 66:469–497.

Mann, S.K.O., P.N. Devreotes, S. Eliott, K. Jermyn, A. Kuspa, M. Fechheimer, R. Furukawa, C.A. Parent, J. Segall, G. Shaulsky, et al. 1998. Cell biological, molecular genetic, and biochemical methods to examine *Dictyostelium*. *In* Cell Biology: A Laboratory Handbook. Second edition. J.E. Celis, editor. Academic Press, San Diego. 431–465.

Martin, S.S., and P. Leder. 2001. Human MCF10A mammary epithelial cells undergo apoptosis following actin depolymerization that is independent of attachment and rescued by Bcl-2. *Mol. Cell. Biol.* 21:6529–6536.

Mashima, T., M. Naito, K. Noguchi, D.K. Miller, D.W. Nicholson, and T. Tsuruo. 1997. Actin cleavage by CPP-32/apopain during the development of apoptosis. *Oncogene.* 14:1007–1012.

Mills, J.C., N.L. Stone, J. Erhardt, and R.N. Pittman. 1998. Apoptotic membrane blebbing is regulated by myosin light chain phosphorylation. *J. Cell Biol.* 140:627–636.

Morris, H.R., G.W. Taylor, M.S. Masento, K.A. Jermyn, and R.R. Kay. 1987. Chemical structure of the morphogen differentiation inducing factor from *Dictyostelium discoideum. Nature.* 328:811–814.

Ohtsu, M., N. Sakai, H. Fujita, M. Kashiwagi, S. Gasa, S. Shimizu, Y. Eguchi, Y. Tsujimoto, Y. Sakiyama, K. Kobayashi, and N. Kuzumaki. 1997. Inhibition of apoptosis by the actin-regulatory protein gelsolin. *EMBO J.* 16:4650–4656.

Olie, R.A., F. Durrieu, S. Cornillon, G. Loughran, J. Gross, W.C. Earnshaw, and P. Golstein. 1998. Apparent caspase independence of programmed cell death in *Dictyostelium. Curr. Biol.* 8:955–958.

Porn-Ares, M.I., A. Samali, and S. Orrenius. 1998. Cleavage of the calpain inhibitor, calpastatin, during apoptosis. *Cell Death Differ.* 5:1028–1033.

Schwartz, L.M., S.W. Smith, M.E.E. Jones, and B.A. Osborne. 1993. Do all programmed cell deaths occur via apoptosis? *Proc. Natl. Acad. Sci. USA.* 90: 980–984.

Searle, J., J.F.R. Kerr, and C.J. Bishop. 1982. Necrosis and apoptosis: distinct modes of cell death with fundamentally different significance. *Pathol. Annu.* 17:229–259.

Sebbagh, M., C. Renvoize, J. Hamelin, N. Riche, J. Bertoglio, and J. Breard. 2001. Caspase-3-mediated cleavage of ROCK I induces MLC phosphorylation and apoptotic membrane blebbing. *Nat. Cell Biol.* 3:346–352.

Shi, Y. 2002. Mechanisms of caspase activation and inhibition during apoptosis. *Mol. Cell.* 9:459–470.

Sobolewski, A., N. Neave, and G. Weeks. 1983. The induction of stalk cell differentiation in submerged monolayers of *Dictyostelium discoideum.* Characterization of the temporal sequence for the molecular requirements. *Differentiation.* 25:93–100.

Song, Q.Z., T. Wei, S. Lees-Miller, E. Alnemri, D. Watters, and M.F. Lavin. 1997. Resistance of actin to cleavage during apoptosis. *Proc. Natl. Acad. Sci. USA.* 94:157–162.

Sussman, M. 1987. Cultivation and synchronous morphogenesis of *Dictyostelium* under controlled experimental conditions. *In* Methods in Cell Biology. J.A. Spudich, editor. Harcourt Brace Jovanovich, New York. 9–29.

Sutoh, K. 1993. A transformation vector for *Dictyostelium discoideum* with a new

selectable marker *bsr*. *Plasmid.* 30:150–154.

Syntichaki, P., K. Xu, M. Driscoll, and N. Tavernarakis. 2002. Specific aspartyl and calpain proteases are required for neurodegeneration in *C. elegans*. *Nature.* 419:939–944.

Thompson, C.R.L., and R.R. Kay. 2000. The role of DIF-1 signaling in *Dictyostelium* development. *Mol. Cell.* 6:1509–1514.

Town, C.D., J.D. Gross, and R.R. Kay. 1976. Cell differentiation without morphogenesis in *Dictyostelium discoideum*. *Nature.* 262:717–719.

Uren, A.G., K. O'Rourke, L. Aravind, M.T. Pisabarro, S. Seshagiri, E.V. Koonin, and V.M. Dixit. 2000. Identification of paracaspases and metacaspases. Two ancient families of caspase-like proteins, one of which plays a key role in MALT lymphoma. *Mol. Cell.* 6:961–967.

Villa, P., W. Henzel, M. Sensenbrenner, C. Henderson, and B. Pettmann. 1998. Calpain inhibitors, but not caspase inhibitors, prevent actin proteolysis and DNA fragmentation during apoptosis. *J. Cell Sci.* 111:713–722.

Whittingham, W.F., and K.B. Raper. 1960. Non-viability of stalk cells in *Dictyostelium*. *Proc. Natl. Acad. Sci. USA.* 46:642–649.

Xu, K., N. Tavernarakis, and M. Driscoll. 2001. Necrotic cell death in *C. elegans* requires the function of calreticulin and regulators of Ca^{2+} release from the endoplasmic reticulum. *Neuron.* 31:957–971.

Yoshida, K., and K. Inouye. 2001. Myosin II-dependent cylindrical protrusions induced by quinine in *Dictyostelium*: antagonizing effects of actin polymerization at the leading edge. *J. Cell Sci.* 114:2155–2165.

Zakeri, Z., W. Bursch, M. Tenniswood, and R.A. Lockshin. 1995. Cell death: programmed, apoptosis, necrosis, or other? *Cell Death Differ.* 2:87–96.